

Activation of Snap-Top Capped Mesoporous Silica Nanocontainers Using Two Near-Infrared Photons

Tania M. Guardado-Alvarez, Lekshmi Sudha Devi, Melissa M. Russell, Benjamin J. Schwartz, and Jeffrey I. Zink*

Department of Chemistry and Biochemistry and California NanoSystems Institute, University of California, Los Angeles, California 90095-1569, United States

S Supporting Information

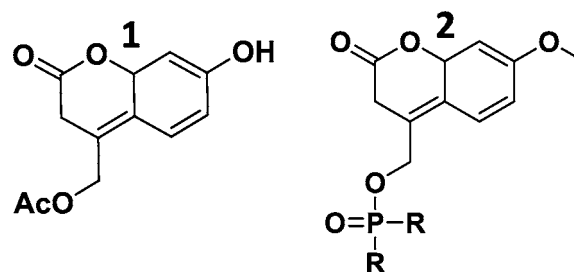
ABSTRACT: Photoactivation of “snap-top” stoppers over the pore openings of mesoporous silica nanoparticles releases intact cargo molecules from the pores. The on-command release can be stimulated by either one UV photon or two coherent near-IR photons. Two-photon activation is particularly desirable for use in biological systems because it enables good tissue penetration and precise spatial control. Stoppers were assembled by first binding photolabile coumarin-based molecules to the nanoparticle surface. Then, after the particles were loaded with cargo, bulky β -cyclodextrin (CD) molecules were noncovalently associated with the substituted coumarin molecule, blocking the pores and preventing the cargo from escaping. One-photon excitation at 376 nm or two-photon excitation at 800 nm cleaves the bond holding the coumarin to the nanopore, releasing both the CD cap and the cargo. The dynamics of both the cleavage of the cap and the cargo release was monitored using fluorescence spectroscopy. This system traps intact cargo molecules without the necessity of chemical modification, releases them with tissue-penetrating near-IR light, and has possible applications in photostimulated drug delivery.

A rapidly developing area of nanomedicine is stimuli-responsive on-command drug delivery using nanoparticle carriers; the ultimate goal is to deliver a high local concentration of a therapeutic agent with no premature release. Light-activated delivery offers the possibility of precise spatial localization¹ of the release and also of the timing of the drug delivery.^{1–8} A limitation is the depth of tissue penetration of the light; the best transmission occurs with near-IR light at wavelengths of 750–800 nm.^{4,8,9} Researchers are thus increasingly focusing attention on coherent two-photon excitation to achieve excitation energies to activate the release.^{4–8,10} An important line of research has been prodrug motifs in which a drug molecule is chemically bonded to a carrier molecule or particle and is photochemically cleaved from the carrier.¹¹ A major disadvantage with this approach, however, is that chemical modification of the original drug is required in order to attach it to a photolabile group. This creates many difficulties because the prodrug has to be biocompatible and it must give the active drug as a result of the cleavage. Creating a prodrug is lengthy and costly because of both screening requirements of the prodrug for toxicity and

the need for a new synthetic technique for each drug that is used.^{11,12} The use of a prodrug grafted on silica nanoparticles has been reported,¹² although this particular example still has the same limitations as any other prodrug.

Within the past decade, mesoporous silica nanoparticles (MSNs) have increased in popularity for drug delivery purposes, in part because intact drug molecules can be stored in the pores. MSNs also have been shown to be nontoxic in multiple *in vivo* studies and have been proven to hold a wide variety of drugs.¹⁴ MSNs possess other advantages such as ease of functionalization, a robust framework, and little to no biotoxicity.^{3,14–17} Commonly used functionalizations include attachment of polymers to the outer surface,^{14,18} incorporation of molecules into the framework,^{3,7,14,19} and attachment of molecules including nanomachines around the pore openings.^{15,16,20,21} The latter derivatized particles can deliver drugs using various stimuli.¹³ Several examples of photoactivated^{2–4,6,7,22–24} drug release from MSNs and “snap-top”^{14,21,25,26} caps have been reported. These include a coumarin-based system that when dimerized has the ability to act as a gatekeeper, blocking the MSN pores;²³ photodissociation of β -cyclodextrin (CD) from a derivatized azobenzene to unblock the pores;³ and photocleavage of the N–C bond of an *o*-methoxybenzylamine-based gatekeeper.²⁶ All of these previous studies used single-photon excitation in the visible/near-UV region of the spectrum. In this Communication, we describe a system that utilizes MSNs of the MCM-41 type and a 7-hydroxy-4-(hydroxymethyl)-3,8a-hydro-2*H*-chromen-2-one (**1**, Scheme 1) as the basis for a snap-top that can be released with either one- or two-photon

Scheme 1. Photocleavable Coumarin Derivations



Received: March 20, 2013

Revised: July 19, 2013

Published: September 9, 2013

activation for use in drug delivery (Figure 1). Because the MSN pores are chemically inert, drug molecules can be stored in the

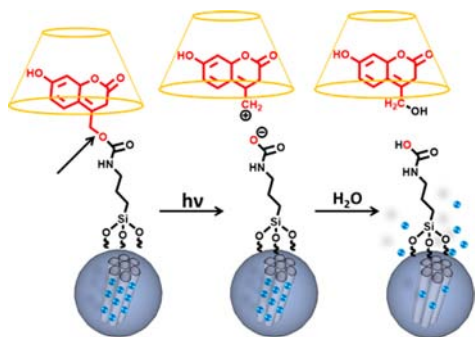


Figure 1. Photocleavage mechanism of the snap-top cap. Final products are shown on the right.

pores without chemical modification, and the release can be performed with near-IR light that is at the optimal wavelength for tissue penetration.

The system we discuss in this Communication is based on photocleavage of the C–O bond shown in Figure 1. This photolabile protecting group was reported to have a two-photon cross-section of ~ 1.07 GM at 740 nm and 0.13 GM at 800 nm (measured for **1**);²⁴ when excited by one or two photons, the C–O bond is cleaved, creating a carbocation that is subsequently hydrolyzed. The mechanism for the photocleavage was described by Furuta et al. for **2** (Scheme 1), and a similar mechanism likely operates for the one- and two-photon cleavage of **4**.²⁷ The MSNs used in this work were synthesized as previously reported in the literature.^{14,28} The pore structure of the nanoparticles was confirmed using powder X-ray diffraction (PXRD) and transmission electron microscopy (TEM) (Figure 2). From the TEM studies the pore diameter

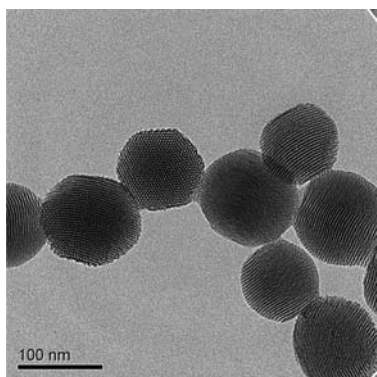


Figure 2. TEM image of MSNs after surfactant extraction. Scale bar, 100 nm.

was calculated to be about 2.5 nm and the particle size about 100 nm. From the PXRD the higher order peaks observed can be indexed as the (1 0 0), (1 1 0), and (2 0 0) planes with a lattice spacing of 4 nm (Supporting Information (SI)). The N_2 absorption/desorption isotherms showed a specific surface of 1044 m^2/g (SI). Commercially available 7-hydroxy-4-(chloromethyl)-3,8a-hydro-2H-chromen-2-one was hydrolyzed to yield **3**. It was reacted with 3-(triethoxysilyl)propyl isocyanate to generate **4** (Figure 3) which was then condensed on the surface of the silica nanoparticles. The attachment of **4** on the

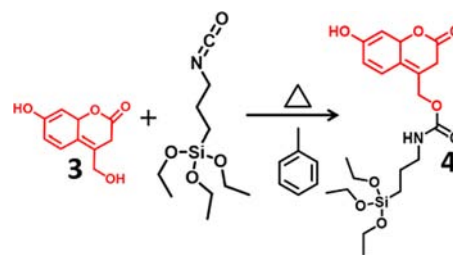


Figure 3. Synthesis of the silane-modified coumarin molecule.

surface of the nanoparticles was confirmed using IR, UV/vis, and solid-state NMR spectroscopy. The IR spectrum showed a peak at ~ 1600 cm^{-1} indicating the presence of a carbonyl stretch attributed to the lactone functional group. The ^{13}C solid-state NMR shows chemical shifts at 160 ppm for the carbonyl carbon as well as the peaks corresponding to the aromatic region around 110 ppm (SI). The ^{29}Si solid-state NMR showed chemical shifts at -91 , -101 , and -110 ppm corresponding to the silica framework and -66 ppm corresponding to the functionalization shift (SI). The UV/vis of the particles in solution showed the absorption peak of **4**. After the attachment, the particles were soaked in a concentrated solution of Rhodamine B, which serves as the “cargo” and incorporates into the pores by diffusion. CD was added to the solution, which associates with **4** due to hydrophobic interactions. Due to its size, CD blocks the pore openings and thus traps the chemically unmodified Rhodamine B cargo molecules inside the pores. Previous *in vitro* studies show that CD hydrophobic associations are not affected by biomolecules.¹⁴

The operation of the light-activated snap-top system was monitored by measuring the amount of Rhodamine B cargo released from the particles into solution using fluorescence spectroscopy. The nanoparticles were placed into one corner of a cuvette to which deionized water was carefully added. The opposite corner contained a small stir bar operated at a low speed to disperse released molecules with minimal disturbance to the particles (SI). The concentration of the released molecules in the solution above the particles was measured at 1-s time intervals by fluorescence spectroscopy using 408-nm laser excitation. We simultaneously monitored the fluorescence intensity of the released Rhodamine B cargo at 580 nm and that of the dissociated cap, which contains fragment **3**, at 490 nm. The flat baseline measured at both wavelengths before the system was irradiated shows that there is insignificant leakage from the capped pores. The fluorescence intensity increased after activation of the snap-top because the molecules left the particles and diffused into solution.

The results of our release measurements are shown in Figure 4. The fluorescence intensity remained within the background when the pump laser was off, showing that the cap remains bonded to the particles and that there is no leakage of the cargo. After verifying that there was no change in fluorescence intensity for 2 h, we then applied 376-nm excitation light to the sample. This has the effect of cleaving the bond indicated by the arrow in Figure 1, which in turn uncaps the pores, allowing both the cap and the cargo to escape into solution. Immediately after activation, an increase in fluorescence intensity of both the cap and the Rhodamine B cargo was observed. As expected, the release of the cap was observed to occur at a faster rate than that of the cargo because diffusion of the cargo out of the 2.5-nm pores is a slower process, particularly given the favorable

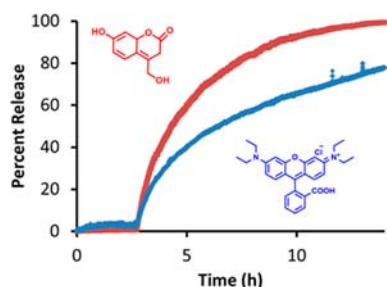


Figure 4. Release profiles of cap (red) and Rhodamine B cargo (blue). The probe laser is on continuously. The 376-nm pump laser is turned on after 2.5 h.

electrostatic interaction of Rhodamine B with the walls of the silica pores. We calculated the released amount of Rhodamine B cargo after 14 h of irradiation to be 1.6 wt%. To quantify the total amount of Rhodamine B released by irradiation, we stirred the solution for an extra 16 h in the dark to allow any leftover Rhodamine B to diffuse out into solution. We then measured the UV/vis absorbance, which yielded a released amount of Rhodamine B cargo of 2.3 wt%.

To prove that the cleavage and cargo release resulted from a photochemical reaction and not a thermal process caused by local laser heating, we conducted two control experiments. First, we carried out the same release detection measurements while externally heating the sample without any laser excitation. In this experiment, we first monitored the emission for 2 h to verify that no cap dissociation occurred. We then heated the solution to 70 °C and found no increase in fluorescence intensity, verifying that the capping system remained stable. Finally, after about 4.5 h, we turned on the 376-nm pump laser (0.025 W/cm²) and saw that the fluorescence intensity of the cap immediately increased, showing that the system retained its phototriggered capability. Second, in a separate experiment, we irradiated the particles with a high laser power (0.125 W/cm²) at 514 nm where the photocleavable group does not absorb. We also saw no release of the cargo in this experiment, verifying that absorption of a photon with a wavelength that can initiate cleavage of the stopper is necessary for the cargo release. Together, these two experiments prove that the activation of the snap-top and the on-command release of the cargo are caused by a photochemical reaction and not by a thermal process.

We then investigated the activation of the snap-top by two-photon excitation, which we did using the output of an amplified Ti:sapphire laser, which consisted of 40-fs, 60- μ J pulses centered around 800 nm at a repetition rate of 1 kHz. The 800-nm light is also not absorbed by the photocleavable system, so a two (or greater)-photon process is required for this choice of photolysis wavelength. We focused the beam to a 2.5-mm spot size at 0.2 W/cm². Since the ultrafast laser system was not compatible with *in situ* fluorescence monitoring, we slightly modified the way we performed the cargo release measurements for these experiments. We set up the cuvette in the same manner as for the one-photon experiments but then irradiated the samples with the 800-nm light for a series of fixed time intervals. After each interval, we took aliquots of the supernatant containing the released cargo and cap molecules, measured the fluorescence intensity, and then returned the aliquots to the cuvette prior to further irradiation (SI). The release profiles shown in Figure 5 are plots of the fluorescence intensities of the released cap at 490 nm (SI) and Rhodamine B

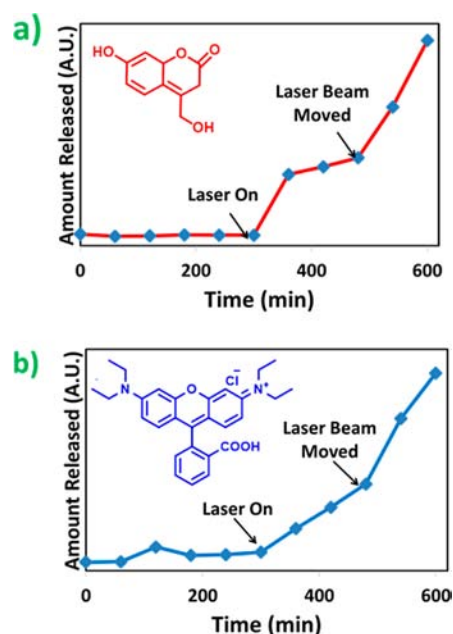


Figure 5. (a) Release profile showing the fluorescence intensity increase of the cap. (b) Release profile showing the fluorescence intensity increase of the Rhodamine B cargo. In both release profiles excitation with 800-nm femtosecond laser pulses was used. The fluorescence intensity of the aliquots was taken every hour.

at 580 nm (SI) at 1-h intervals instead of the 1-s intervals used in the one-photon experiments shown in Figure 4.

The release profiles for two-photon activation shown in Figure 5 verify that the snap-top can be successfully activated by near-IR light. As before, in the absence of the pump laser excitation, the flat baseline (no fluorescence intensity increase over time) shows that no leakage occurs. The 800-nm excitation light was turned on after 5 h, producing an immediate increase in the fluorescence of both the cap and the Rhodamine B cargo. The release efficiency during these two-photon experiments appeared similar to that in the one-photon experiments. Unfortunately, we could not calculate the weight percent of cargo released in these experiments because the laser in the two-photon experiments was focused to a spot that was smaller than the size of the aggregated MSNs, and only a fraction of the particles was excited at a given moment. Figure 5 shows that, after 500 min, the cleavage of the cap was nearing completion, but when the laser beam was moved to a different spot, the release rate started increasing again. Thus, since the release rate is similar to that in the one-photon case, if all of the particles were two-photon irradiated simultaneously, we would anticipate the same weight percent release of cargo as in the one-photon case.

In summary, we have synthesized a photocleavable snap-top based on molecule 3 that can be activated using either one- or two-photon absorption. The two-photon capabilities of this photocleavable snap-top are highly beneficial for biological purposes. The near-IR light will be able to achieve deeper tissue penetration, activation will cause little to no tissue damage, and the method has the additional benefit of precise focal control, all of which make this system ideal for photoactivated cancer therapy without the need to chemically modify a drug.

■ ASSOCIATED CONTENT

● Supporting Information

PXRD, TEM, BET, ^{13}C and ^{29}Si solid-state NMR, UV/vis, IR, release profile with a 514-nm wavelength pump laser, and release profile by external heating. This material is available free of charge via the Internet at <http://pubs.acs.org>.

■ AUTHOR INFORMATION

Corresponding Author

zink@chem.ucla.edu

Notes

The authors declare no competing financial interest.

■ ACKNOWLEDGMENTS

This work was made possible by grants from the NIH RO1 CA133697, the Partner University Fund FACE-PUF 200991853, and NIH fellowship to T.M.G.-A. (CA133697).

■ REFERENCES

- (1) Alvarez-Lorenzo, C.; Bromberg, L.; Concheiro, A. *Photochem. Photobiol.* **2009**, *85*, 848–860.
- (2) Azagarsamy, M. A.; Alge, D. L.; Radhakrishnan, S. J.; Tibbitt, M. W.; Anseth, K. S. *Biomacromolecules* **2012**, *13*, 2219–2224.
- (3) Ferris, D. P.; Zhao, Y. L.; Khashab, N. M.; Khatib, H. A.; Stoddart, J. F.; Zink, J. I. *J. Am. Chem. Soc.* **2009**, *131*, 1686–1688.
- (4) (a) Dai, Y.; Ma, P.; Cheng, Z.; Kang, X.; Zhang, X.; Hou, Z.; Li, C.; Yang, D.; Zhai, X.; Lin, J. *ACS Nano* **2012**, *6*, 3327–3338. (b) Gai, S.; Yang, P.; Li, C.; Wang, W.; Dai, Y.; Niu, N.; Lin, J. *Adv. Funct. Mater.* **2010**, *20*, 1166–1172.
- (5) Bhawalkar, J. D.; Kumar, N. D.; Zhao, C. F.; Prasad, P. N. *J. Clin. Laser Med. Surg.* **1997**, *15*, 201–204.
- (6) Chang, Y. T.; Liao, P. Y.; Sheu, H. S.; Tseng, Y. J.; Cheng, F. Y.; Yeh, C. S. *Adv. Mater.* **2012**, *24*, 3309–3314.
- (7) Choi, S. K.; Thomas, T.; Li, M. H.; Kotlyar, A.; Desai, A.; Baker, J. R., Jr. *Chem. Commun.* **2010**, *46*, 2632–2634.
- (8) Kim, S.; Ohulchanskyy, T. Y.; Pudavar, H. E.; Pandey, R. K.; Prasad, P. N. *J. Am. Chem. Soc.* **2007**, *129*, 2669–2675.
- (9) Starkey, J. R.; Rebane, A. K.; Drobizhev, M. A.; Meng, F.; Gong, A.; Elliott, A.; McInnerney, K.; Spangler, C. W. *Clin. Cancer Res.* **2008**, *14*, 6564–6573.
- (10) König, K. *J. Microsc.* **2000**, *200*, 83–104.
- (11) *Prodrugs: Challenges and rewards*; Stella, V., Borchardt, R., Hageman, M., Oliyai, R., Maag, H., Tilley, J., Eds.; Biotechnology: Pharmaceutical Aspects 5; Springer: New York, 2007; pp 35–355.
- (12) (a) Mikat, V.; Heckel, A. *RNA* **2007**, *13*, 2341–2347. (b) Fomina, N.; McFearin, C.; Sermsakdi, M.; Edigin, O.; Almutairi, A. *J. Am. Chem. Soc.* **2010**, *132*, 9540–9542. (c) Rautio, J.; Kumpulainen, H.; Heimbach, T.; Oliyai, R.; Oh, D.; Järvinen, T.; Savolainen, J. *Nat. Rev. Drug Discovery* **2008**, *7*, 255–270.
- (13) Lin, Q.; Huang, Q.; Li, C.; Bao, C.; Liu, Z.; Li, F.; Zhu, L. *J. Am. Chem. Soc.* **2010**, *132*, 10645–10647.
- (14) (a) Li, Z.; Barnes, J. C.; Bosoy, A.; Stoddart, J. F.; Zink, J. I. *Chem. Soc. Rev.* **2012**, *41*, 2590–2605. (b) Ambrogio, M. W.; Thomas, C. R.; Zhao, Y.; Zink, J. I.; Stoddart, J. F. *Acc. Chem. Res.* **2011**, *44*, 903–913. (c) Yang, P.; Gai, S.; Lin, J. *Chem. Soc. Rev.* **2012**, *41*, 3679–3698. (d) Chen, Y.; Chen, H.; Shi, J. *Adv. Mater.* **2013**, *25*, 3144–3176. (e) Meng, H.; Xue, M.; Xia, T.; Zhao, Y.-L.; Tamanoi, F.; Stoddart, J. F.; Zink, J. I.; Nel, A. E. *J. Am. Chem. Soc.* **2010**, *132*, 12690–12697. (f) Lai, J.; Shah, B. P.; Garfunkel, E.; Lee, K.-B. *ACS Nano* **2013**, *7*, 2741–2750.
- (15) Ambrogio, M. W.; Pecorelli, T. A.; Patel, K.; Khashab, N. M.; Trabolsi, A.; Khatib, H. A.; Botros, Y. Y.; Zink, J. I.; Stoddart, J. F. *Org. Lett.* **2010**, *12*, 3304–3307.
- (16) (a) Angelos, S.; Yang, Y. W.; Patel, K.; Stoddart, J. F.; Zink, J. I. *Angew. Chem.* **2008**, *120*, 2254–2258. (b) Angelos, S.; Khashab, N. M.; Yang, Y. W.; Trabolsi, A.; Khatib, H. A.; Stoddart, J. F.; Zink, J. I. *J. Am. Chem. Soc.* **2009**, *131*, 12912–12914.
- (17) (a) Casasús, R.; Climent, E.; Marcos, M. D.; Martínez-Máñez, R.; Sancenón, F.; Soto, J.; Amorós, P.; Cano, J.; Ruiz, E. *J. Am. Chem. Soc.* **2008**, *130*, 1903–1917. (b) DeMuth, P.; Hurley, M.; Wu, C.; Galanie, S.; Zachariah, M. R.; DeShong, P. *Microporous Mesoporous Mater.* **2011**, *141*, 128–134. (c) Thomas, C. R.; Ferris, D. P.; Lee, J. H.; Choi, E.; Cho, M. H.; Kim, E. S.; Stoddart, J. F.; Shin, J. S.; Cheon, J.; Zink, J. I. *J. Am. Chem. Soc.* **2010**, *132*, 10623–10625.
- (18) Zhang, J.; Misra, R. D. K. *Acta Biomater.* **2007**, *3*, 838–850.
- (19) Lin, Y. S.; Tsai, C. P.; Huang, H. Y.; Kuo, C. T.; Hung, Y.; Huang, D. M.; Chen, Y. C.; Mou, C. Y. *Chem. Mater.* **2005**, *17*, 4570–4573.
- (20) (a) Angelos, S.; Liong, M.; Eunchil, C.; Zink, J. I. *Chem. Eng. J.* **2008**, *137*, 4–13. (b) Zhao, Y.; Li, Z.; Kabehie, S.; Botros, Y. Y.; Stoddart, J. F.; Zink, J. I. *J. Am. Chem. Soc.* **2010**, *132*, 13016–13025. (c) Wang, C.; Li, Z.; Cao, D. *Angew. Chem., Int. Ed.* **2012**, *51*, 5460–5465.
- (21) Patel, K.; Angelos, S.; Dichtel, W. R.; Coskun, A.; Yang, Y. W.; Zink, J. I.; Stoddart, J. F. *J. Am. Chem. Soc.* **2008**, *130*, 2382–2383.
- (22) (a) Kumar, S.; Allard, J.-F.; Morris, D.; Dory, Y. L.; Lepage, M.; Zhao, Y. *J. Mater. Chem.* **2012**, *22*, 7252–7257. (b) Lu, J.; Choi, E.; Tamanoi, F.; Zink, J. I. *Small* **2008**, *4*, 421–426. (c) Park, C.; Lee, K.; Kim, C. *Angew. Chem.* **2009**, *121*, 1301–1304. (d) Park, C.; Oh, K.; Lee, S. C.; Kim, C. *Angew. Chem., Int. Ed.* **2007**, *46*, 1455–1457. (e) Schloßbauer, A.; Sauer, A. M.; Cauda, V.; Schmidt, A.; Engelke, H.; Rothbauer, U.; Zolghadr, K.; Leonhardt, H.; Bräuchle, C.; Bein, T. *Adv. Healthcare Mater.* **2012**, *1*, 316–320. (f) Shamay, Y.; Adar, L.; Ashkenasy, G.; David, A. *Biomaterials* **2011**, *32*, 1377–1386. (g) Sun, L.; Yang, Y.; Dong, C. M.; Wei, Y. *Small* **2011**, *7*, 401–406. (h) Yang, Y.; Song, W.; Wang, A.; Zhu, P.; Fei, J.; Li, J. *Phys. Chem. Chem. Phys.* **2010**, *12*, 4418–4422. (i) Saha, S.; Johansson, E.; Flood, A. H. *Chem.—Eur. J.* **2005**, *11*, 6846–6858.
- (23) Mal, N. K.; Fujiwara, M.; Tanaka, Y. *Nature* **2003**, *421*, 350–353.
- (24) Furuta, T.; Wang, S. S.-H.; Dantzker, J. L.; Dore, T. M.; Bybee, W. J.; Callaway, E. M.; Denk, W.; Tsien, R. Y. *Proc. Natl. Acad. Sci. U.S.A.* **1999**, *96*, 1193–1200.
- (25) (a) Vivero-Escoto, J. L.; Slowing, I. I.; Wu, C. W.; Lin, V. S. Y. *J. Am. Chem. Soc.* **2009**, *131*, 3462–3463. (b) Lai, C.-Y.; Trewyn, B. G.; Jeftinija, D. M.; Jeftinija, K.; Xu, S.; Jeftinija, S.; Lin, V. S. Y. *J. Am. Chem. Soc.* **2003**, *125*, 4451–4459.
- (26) Agostini, A.; Sancenón, F.; Martínez-Máñez, R.; Marcos, M. D.; Soto, J.; Amorós, P. *Chem.—Eur. J.* **2012**, *18*, 12218–12221.
- (27) Furuta, T.; Iwamura, M. *Methods Enzymol.* **1998**, *291*, 50–63.
- (28) (a) Meng, H.; Xue, M.; Xia, T.; Ji, Z.; Tarn, D. Y.; Zink, J. I.; Nel, A. E. *ACS Nano* **2011**, *5*, 4131–4144. (b) Liong, M.; Lu, J.; Kovoichich, M.; Xia, T.; Ruehm, S. G.; Nel, A. E.; Tamanoi, F.; Zink, J. I. *ACS Nano* **2008**, *2*, 889–896. (c) Kresge, C. T.; Leonowicz, M. E.; Roth, W. J.; Vartuli, J. C.; Beck, J. S. *Nature* **1992**, *359*, 710–712.